

## Electronic Supplementary Information

### Ultrafine PtCo Alloy Nanoparticles Integrated into Porous N-Doped Nanosheets for Durable Oxygen Reduction Reaction

Baoliang Chen <sup>a, b</sup>, Lei Zhao <sup>b</sup>, Zhaozhao Zhu <sup>b</sup>, Pei Xiong <sup>b</sup>, Zhao Li <sup>b</sup>, Jun Song Chen <sup>b, c</sup>, Lanlan Li <sup>a, \*</sup>, Rui Wu <sup>b, \*</sup>

<sup>a</sup> School of Materials Science and Engineering, Hebei University of Technology, Tianjin 300401, China.

<sup>b</sup> School of Materials and Energy, University of Electronic Science and Technology of China, Chengdu 611731, China.

<sup>c</sup> Interdisciplinary Materials Research Center, Institute for Advanced Study, Chengdu University, Chengdu 610106, China.

\*Corresponding authors

E-mail: liabc@hebut.edu.cn (Lanlan Li); ruiwu0904@uestc.edu.cn (Rui Wu)

## 1. Experimental Section

### 1.1. Materials

Zinc acetate dihydrate ( $\text{Zn}(\text{CH}_3\text{COO})_2 \cdot 2\text{H}_2\text{O}$ ) and cobalt acetate tetrahydrate ( $\text{Co}(\text{CH}_3\text{COO})_2 \cdot 4\text{H}_2\text{O}$ ) were sourced from Sinopharm Chemical Reagent Co., Ltd. 2-methylimidazole (98%) was procured from Shanghai Aladdin Biochemical Technology Co., Ltd. Methanol and hydrochloric acid (HCl) were obtained from Chengdu Kelong Chemical Co., Ltd. Dopamine hydrochloride (98%) was purchased from Shanghai Macklin Biochemical Co., Ltd. Chloroplatinic acid hexahydrate ( $\text{H}_2\text{PtCl}_6 \cdot 6\text{H}_2\text{O}$ , 38%). Pt/C catalyst (20wt%, Johnson Matthey) was purchased from Shanghai Hesun Electric Co., Ltd.

### 1.2. Synthesis of the PtCo-CoNC-P catalyst

Typically, 3.936 g of 2-MeIm was dissolved in 80 mL of deionized water and rapidly mixed with a solution containing 100 mg of  $\text{Co}(\text{CH}_3\text{COO})_2 \cdot 4\text{H}_2\text{O}$  and 1.5 g of  $\text{Zn}(\text{CH}_3\text{COO})_2 \cdot 2\text{H}_2\text{O}$  in 30 mL of deionized water. After stirring for 2 hours, the mixture was centrifuged, dried at  $60^\circ\text{C}$ , resulting in a purple Zn/Co-ZIF product.

Next, 400 mg of Zn/Co-ZIF and 100 mg of DA were dispersed in methanol solution (30 mL,  $\text{pH}=8.5$ ) and continuously stirred for 12 h to obtain Zn/Co-ZIF@PDA. The Zn/Co-ZIF@PDA particles were pyrolyzed at  $900^\circ\text{C}$  under an Ar atmosphere for 2 h with a heating rate of  $5^\circ\text{C min}^{-1}$  to obtain the CoNC-P support. After that, 50 mg of CoNC-P was dispersed in 10 mL of  $\text{H}_2\text{PtCl}_6$  solution ( $0.75 \text{ mg}_{\text{Pt}} \text{ mL}^{-1}$ ) and stirred overnight. The above mixture was dried and heated at  $800^\circ\text{C}$  for 2 h with a  $5^\circ\text{C min}^{-1}$  heating rate under an Ar/ $\text{H}_2$  (5%) atmosphere. Finally, the PtCo-CoNC-P catalyst was obtained after HCl (1 M) washing and drying. For comparison, the synthesis of PtCo-CoNC mirrored this process, just replace CoNC-P with CoNC.

### 1.3. Characterization

The catalysts' crystal structures were analyzed using X-ray diffraction (XRD). Surface compositions were examined by X-ray photoelectron spectroscopy (XPS) using Thermo Fisher Scientific Escalab 250Xi equipment. High-resolution transmission electron microscopy (HR-TEM) images were taken on a JEM-2100F device. Advanced analyses using aberration-corrected scanning and transmission electron microscopy (AC-STEM) were performed on a Thermo Fischer Titan G2 60-300. An EDX-GENESIS spectrometer conducted elemental mapping. The Pt content was quantified using inductively coupled plasma mass spectrometry (ICP-MS) on an Agilent 720ES. X-

ray absorption spectroscopy (XAS) was undertaken at the BL14W1 station at the Shanghai Synchrotron Radiation Facility.

#### *1.4. Electrochemical Measurements*

2.0 mg of as-prepared catalyst was ultrasonically dispersed into a mixture of ethanol (790  $\mu\text{L}$ ) and Nafion (10  $\mu\text{L}$ , 5 wt%) to form a homogeneous catalyst ink. This ink was added dropwise onto a glassy-carbon rotating disk electrode (RDE) with a loading of  $17.8 \mu\text{g}_{\text{Pt}} \text{cm}^{-2}$  for PtCo-CoNC-P and PtCo-CoNC,  $25.5 \mu\text{g}_{\text{Pt}} \text{cm}^{-2}$  for Pt/C. Cyclic voltammetry (CV) was performed in  $\text{N}_2$ -saturated 0.1 M  $\text{HClO}_4$  at a scan rate of  $50 \text{ mV s}^{-1}$ . Linear sweep voltammetry (LSV) was conducted in  $\text{O}_2$ -saturated 0.1 M  $\text{HClO}_4$  at 1600 rpm and the sweep rate was  $10 \text{ mV s}^{-1}$ . Accelerated durability tests were performed by repetitive potential cycles between 0.6 and 1.0 V vs. RHE at  $100 \text{ mV s}^{-1}$  for 30000 cycles in  $\text{O}_2$ -saturated electrolyte Chronoamperometry measurements were carried out at a constant potential of 0.7 V vs. RHE in an  $\text{O}_2$ -saturated 0.1 M  $\text{HClO}_4$  solution.

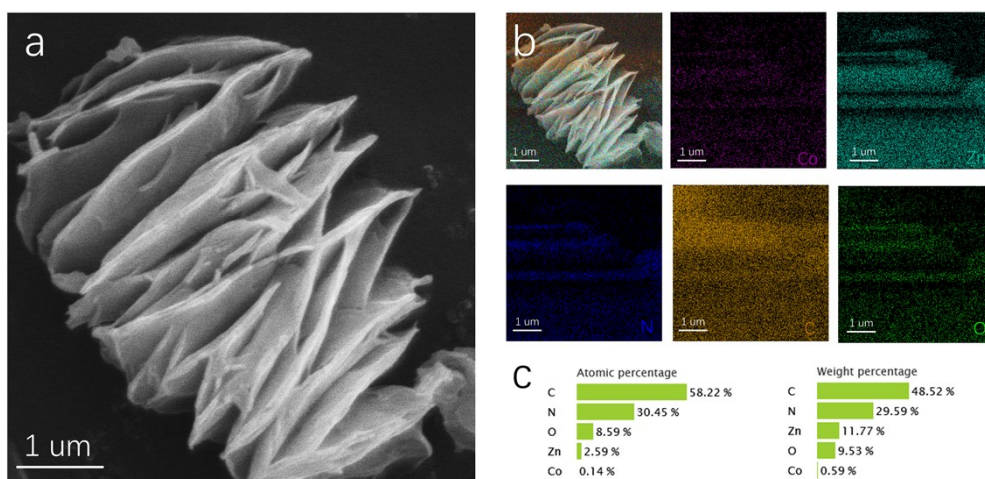


**Fig. S1** (a) SEM images, (b) EDS mapping, and (c) corresponding elemental compositions of Zn/Co-ZIF.

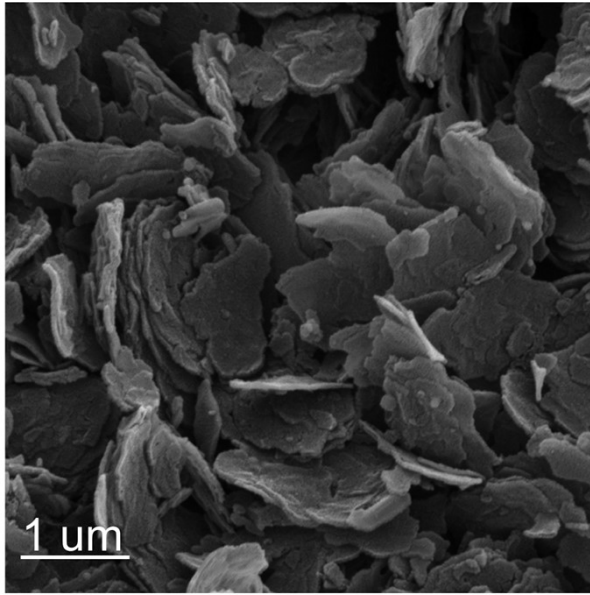


**Fig. S2** SEM image of CoNC-P.

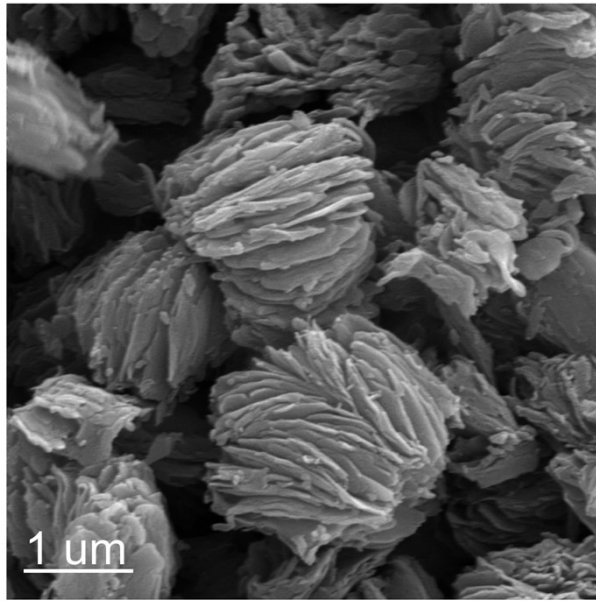


**Fig. S3** SEM image of CoNC.

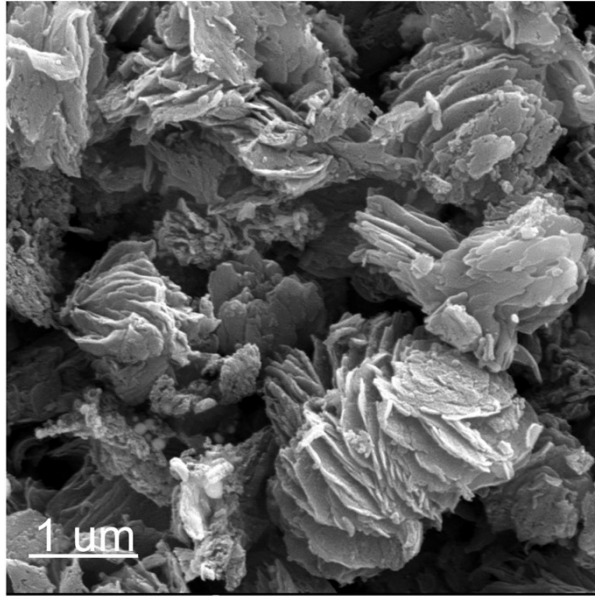


**Fig. S4** SEM image of PtCo-CoNC-P.

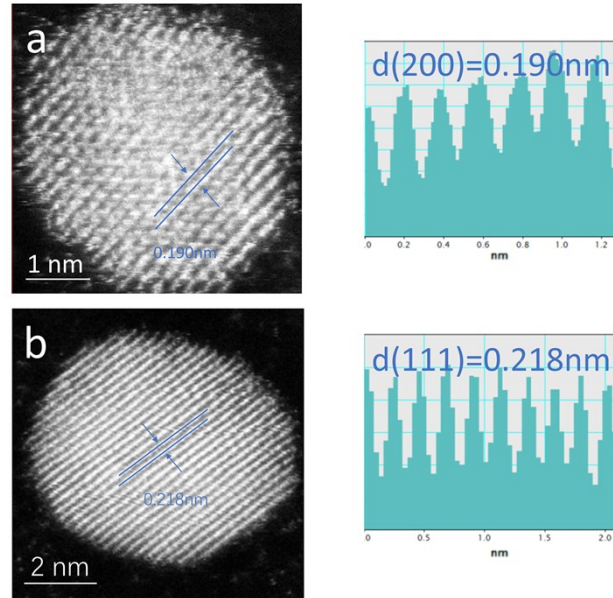


**Fig. S5** (a, b) AC-STEM image of PtCo-CoNC-P and corresponding lattice spacing analysis.

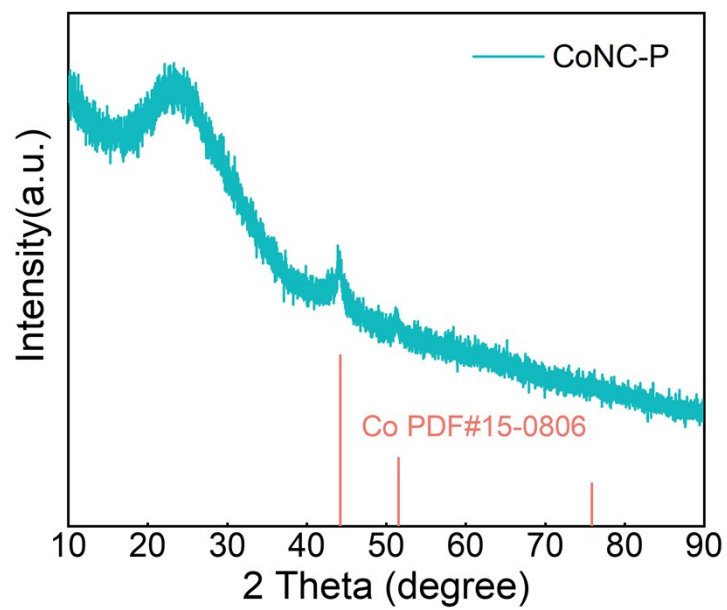


**Fig. S6** XRD pattern of CoNC-P.

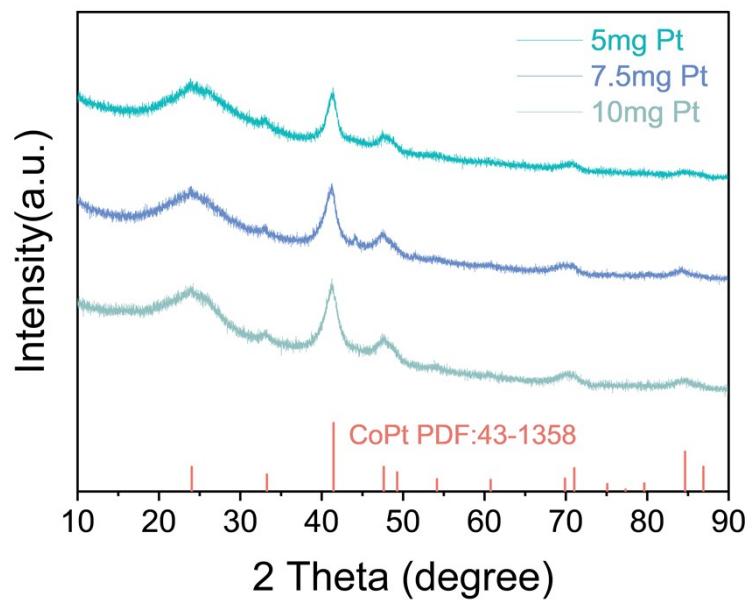


**Fig. S7** XRD spectra of different PtCo-CoNC-P products obtained with different Pt loadings.

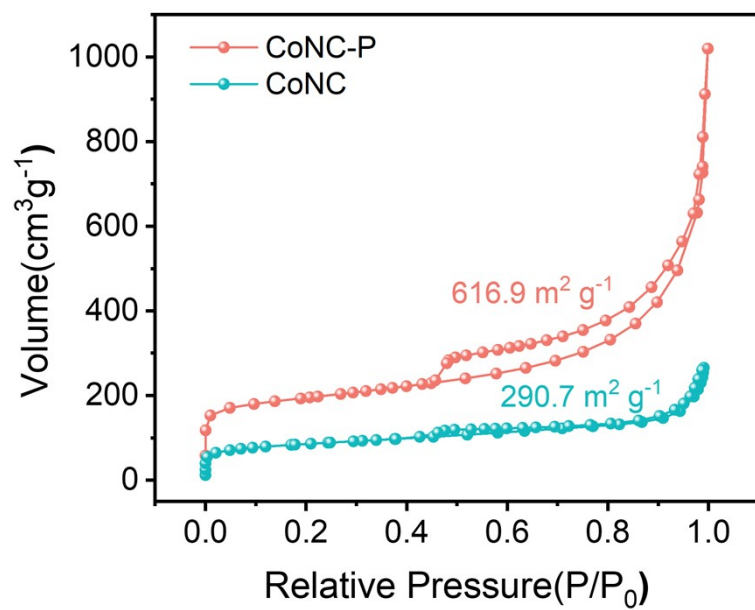


**Fig. S8** N<sub>2</sub> adsorption/desorption isotherms of CoNC-P and CoNC.

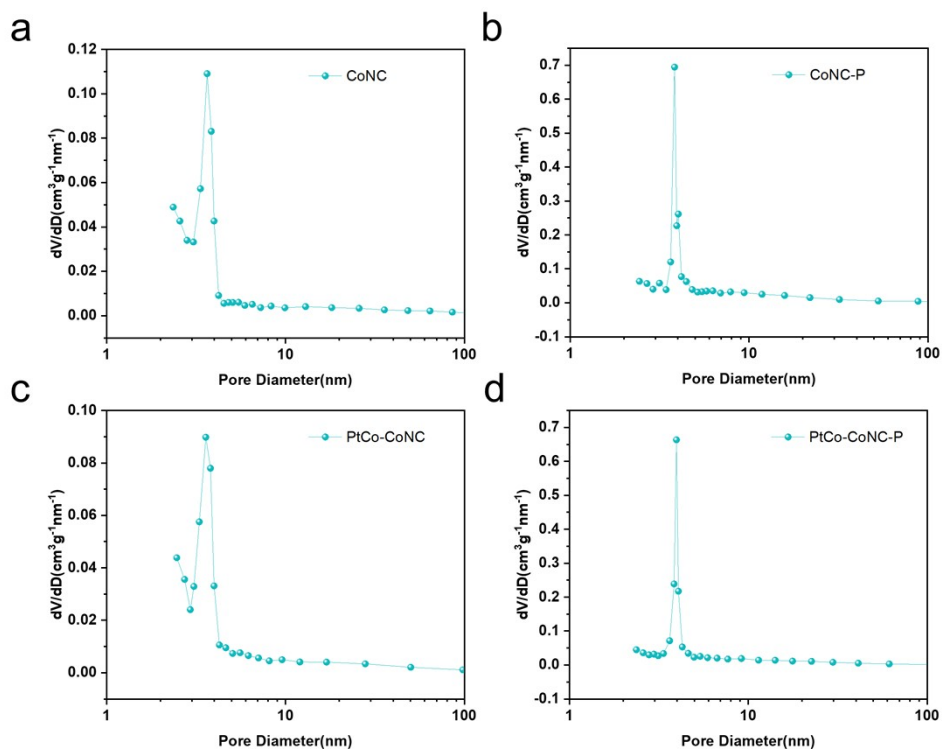


**Fig. S9** The pore size distributions of (a) CoNC (b) CoNC-P (c) PtCo-CoNC and (d) PtCo-CoNC-P.

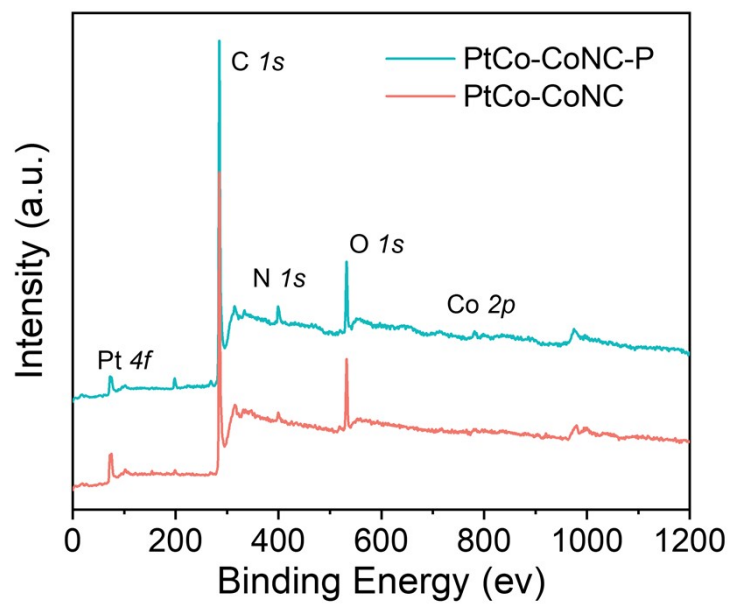


**Fig. S10** XPS survey spectra of PtCo-CoNC-P and PtCo-CoNC.

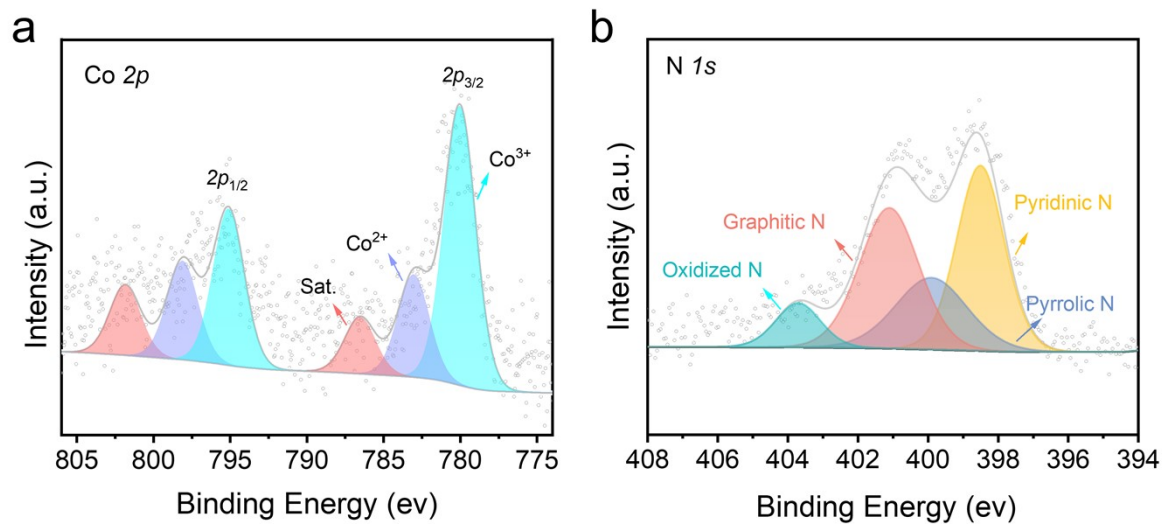


**Fig. S11** High-resolution (a) Co 2p spectrum and (b) N 1s spectrum of PtCo-CoNC-P.

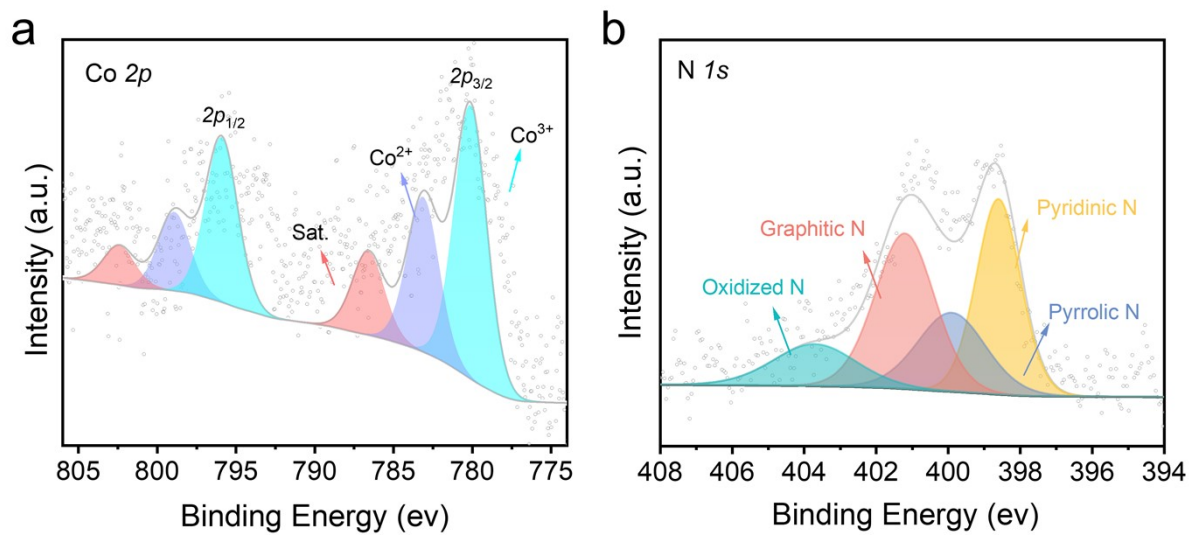


**Fig. S12** High-resolution Co 2p spectrum (a) and high-resolution N 1s spectrum (b) of PtCo-CoNC.

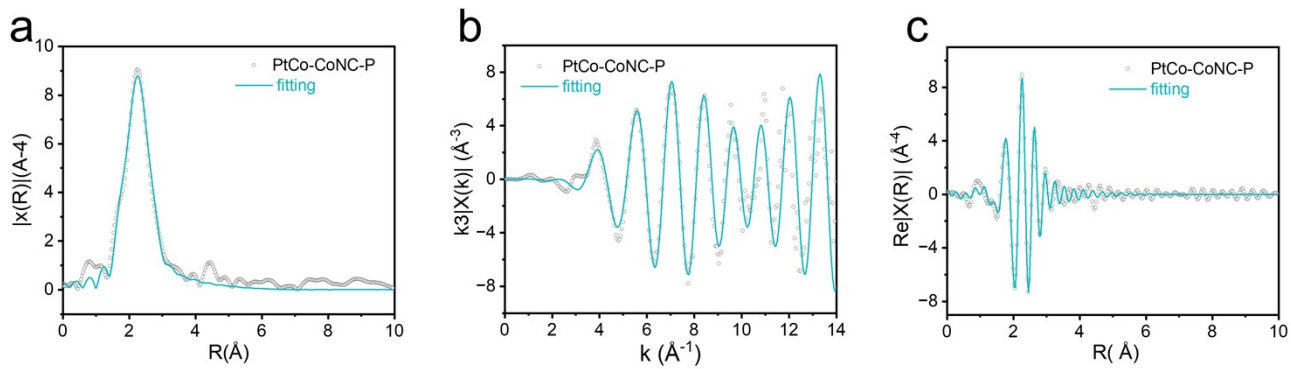


**Fig. S13** FT-EXAFS fitting results of (a) the Pt L3-edge and corresponding  $k$ (b) and  $R$ (c) space fitting results for PtCo-CoNC-P.

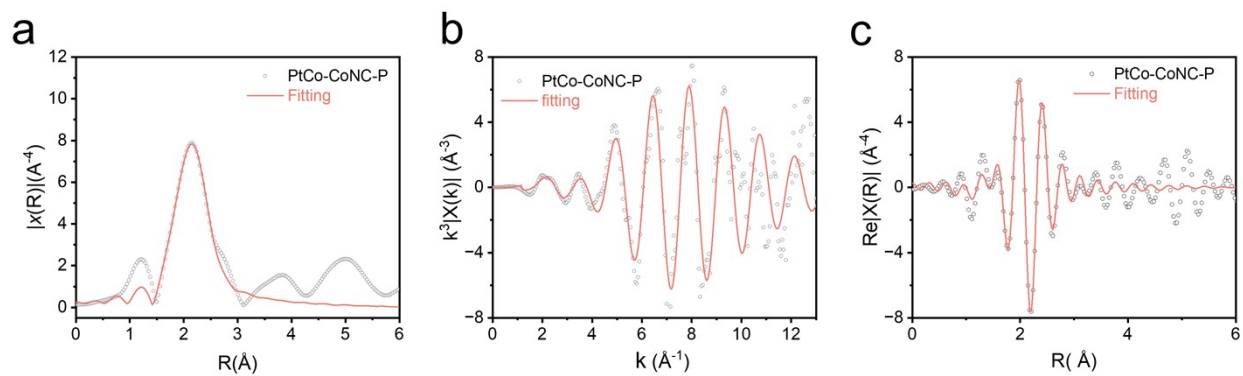


**Fig. S14** FT-EXAFS fitting results (a) of the Co K-edge and corresponding  $k$ (b) and  $R$ (c) space fitting results for PtCo-CoNC-P.

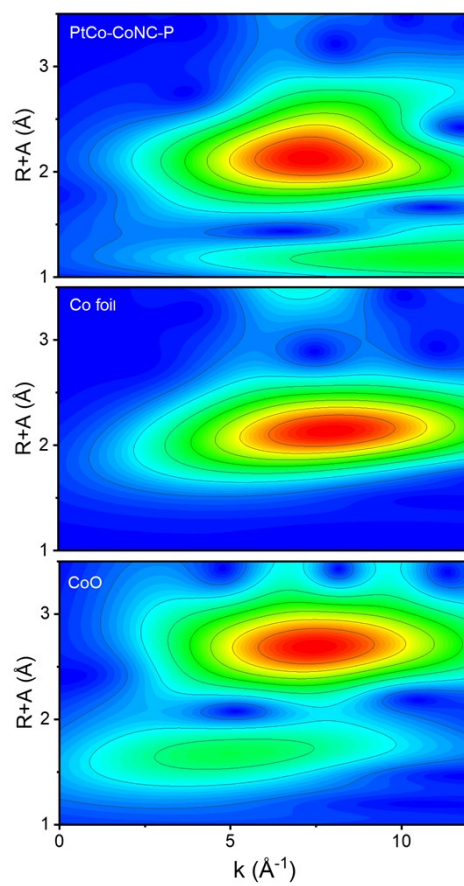


**Fig. S15** Wavelet transform spectra of Co in PtCo-CoNC-P referenced with Co foil and CoO.

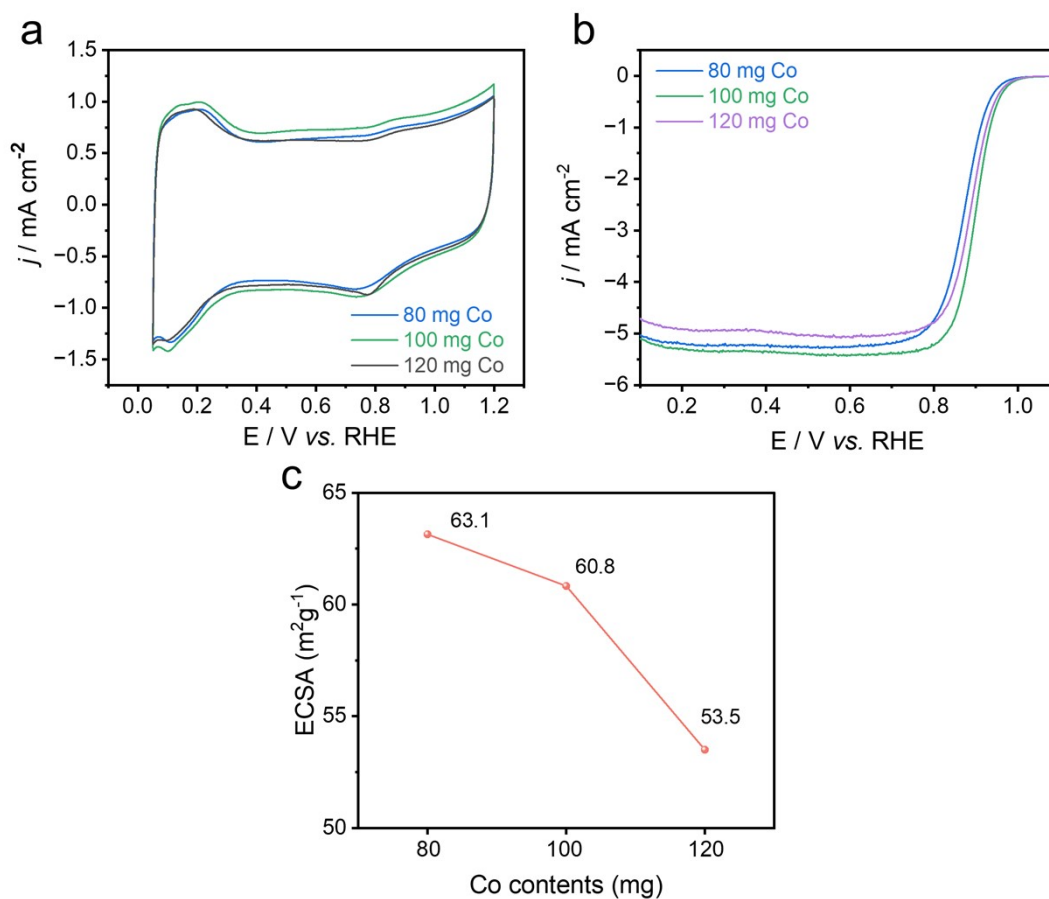


**Fig. S16** (a) CV curves of the PtCo-CoNC-P catalyst prepared with different Co contents in 0.1 M  $\text{HClO}_4$  saturated with  $\text{N}_2$  at a scan rate of  $50 \text{ mV s}^{-1}$ . (b) LSV curves of the PtCo-CoNC-P catalyst prepared with different Co contents in 0.1 M  $\text{HClO}_4$  saturated with  $\text{O}_2$  at 1,600 rpm and a scan rate of  $50 \text{ mV s}^{-1}$ . (c) ECSA comparison of different PtCo-CoNC-P products.

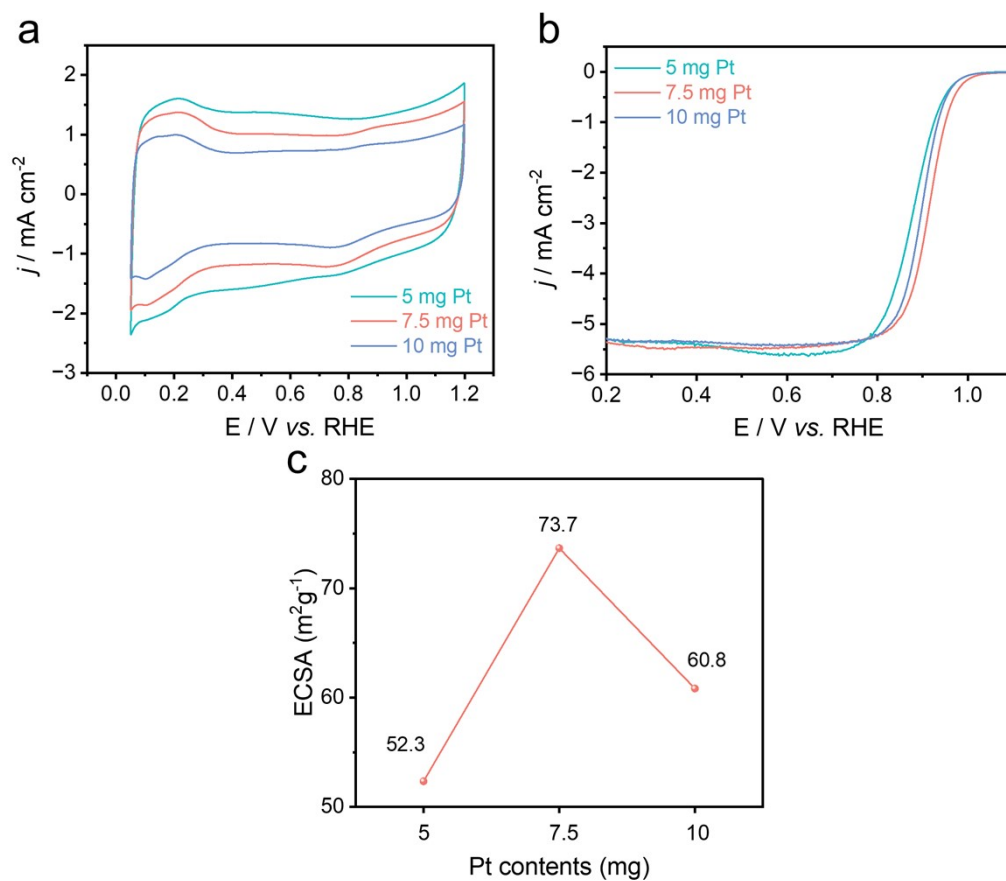


**Fig. S17** (a) CV curves of the PtCo-CoNC-P catalyst prepared with different Pt contents in 0.1 M  $\text{HClO}_4$  saturated with  $\text{N}_2$  at a scan rate of  $50 \text{ mV s}^{-1}$ . (b) LSV curves of the PtCo-CoNC-P catalyst prepared with different Co contents in 0.1 M  $\text{HClO}_4$  saturated with  $\text{O}_2$  at 1,600 rpm and a scan rate of  $50 \text{ mV s}^{-1}$ . (c) ECSA comparison of different PtCo-CoNC-P products.

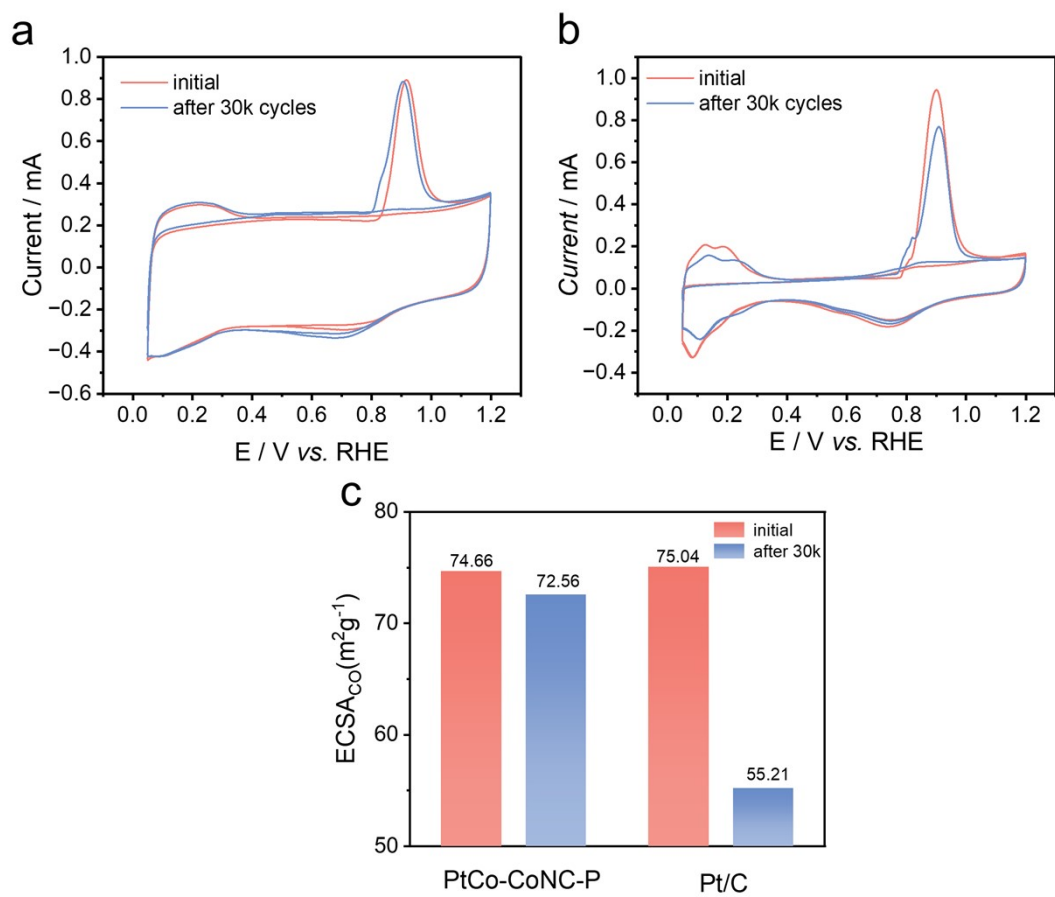


**Fig. S18** CO stripping voltammograms of (a) PtCo-CoNC-P and (b) Pt/C before and after 30,000 cycles, and (c) corresponding ECSA comparison.

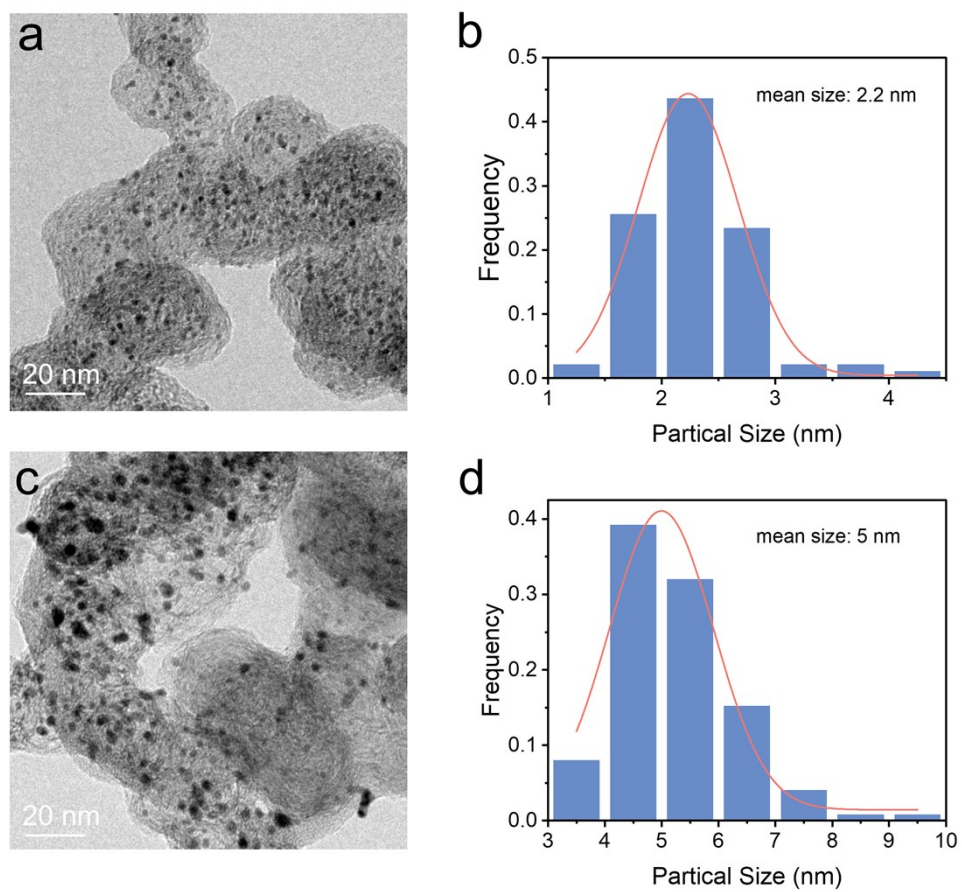


**Fig. S19** TEM images and corresponding Pt NPs size distributions of (a, b) fresh Pt/C catalyst and (c, d) aged Pt/C catalyst after 30,000 cycles.

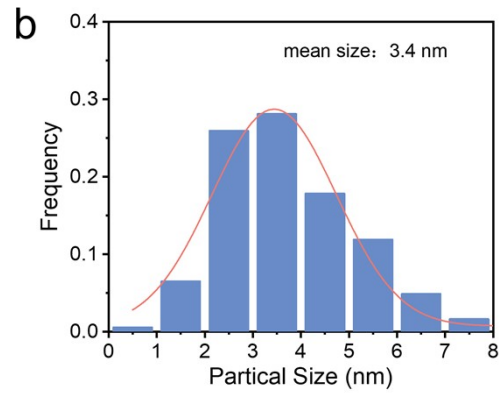
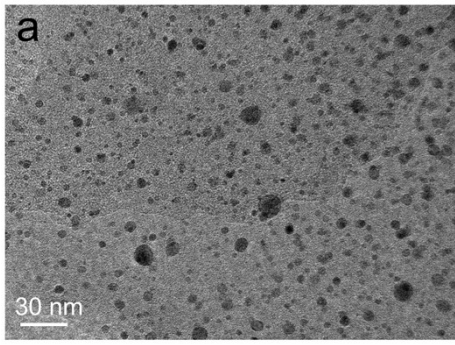


**Fig. S20** TEM image of (a) PtCo-CoNC-P and (b) corresponding size distribution histogram after 30,000 potential cycles.

**Table S1** Pore parameters for PtCo-CoNC-P, PtCo-CoNC, CoNC-P and CoNC.

Sample	PtCo-CoNC-P	CoNC-P	PtCo-CoNC	CoNC
Specific surface area (m <sup>2</sup> g <sup>-1</sup> )	462.5	616.9	257.6	290.0
Average pore size (nm)	3.40	5.11	2.92	2.83
Total pore volume (cm <sup>3</sup> g <sup>-1</sup> )	0.78	1.57	0.35	0.41

**Table S2** Elemental composition determined by XPS for PtCo-CoNC-P and PtCo-CoNC.

Sample	Pt/at%	Co/at%	N/at%	C/at%
PtCo-CoNC-P	0.59	0.42	5.29	93.70
PtCo-CoNC	0.24	0.28	1.46	98.02

**Table S3** Structural parameters extracted from the EXAFS fitting of PtCo-CoNC-P.

Sample	Shell	N <sup>a</sup>	R (Å) <sup>b</sup>	$\sigma^2$ (Å <sup>2</sup> ·10 <sup>-3</sup> ) <sup>c</sup>	$\Delta E^0$ (eV) <sup>d</sup>	R factor (%)
Co foil	Co-Co	12	2.48	6.3±0.3	-3.74±0.5.1	0.22
Pt foil	Pt-Pt	12	2.78	3.9±0.2	7.10±0.37	0.25
PtCo-CoNC-P	Pt-Co	8	2.53	13.5±2.0	-5.79±2.37	1.25
	Pt-Pt	4.0±2.4	2.68	3.2±3.7		
	Co-Co	5.4±2.3	2.51	8.3±2.5	5.43±2.31	1.91
	Co-Pt	8	2.53	2.8±1.8		

N<sup>a</sup>: coordination number; R<sup>b</sup>: bond distance;  $\sigma^{2c}$ : Debye-Waller factor;  $\Delta E^{0d}$ : inner potential correction. R factor: goodness of fit. S0<sup>2</sup> was set to 0.76, which was obtained from the experimental EXAFS fit of the reference Co foil by fixing CN as the known crystallographic value and was fixed to all the samples. For the Co *K*-edge of PtCo-CoNC-P, the data range was 1.0 < k < 9.5 Å<sup>-1</sup> and 1.5 < R < 3.4 Å. S0<sup>2</sup> was set to 0.75, which was obtained from the experimental EXAFS fit of reference Pt foil by fixing CN as the known crystallographic value and was fixed to all the samples. For the Pt *L*<sub>3</sub>-edge of PtCo-CoNC-P, the data range was 3.0 < k < 11.0 Å<sup>-1</sup> and 1.0 < R < 3.0 Å.

**Table S4** Comparison of durability tests of recently reported Pt electrocatalysts.

Catalyst	Loss of $E_{1/2}$ (mV) after ADTs	Loss of MA after ADTs (%)	References
PtCo-CoNC-P	2(30k)	15.6(30k)	This Work
PtCo3-H600	12(30k)	30(30k)	1
PtCo/Co <sub>9</sub> N	11(30k)	19(30k)	2
D-Pt3Co/C	11(30k)	19.8(30k)	3
PtCo@NGCS/KB- 800	13(30k)	36.5(30k)	4
O-Pt3Co/NC-1100	14(30k)	51.4(30k)	5
PtCo-PtSn/C	20(30k)	27.4(30k)	6
Pt@Fe-NC	12(20k)	14.18(20k)	7
h-PtCo/C@NC	9(10k)	33(10k)	8
Pt <sub>4</sub> Co@NC-900	3(10k)	16(10k)	9
Fct-PtCo/C@PtIr/C	9(10k)	31(10k)	10

## References

1. Z. Wang, X. Yao, Y. Kang, L. Miao, D. Xia and L. Gan, *Adv. Funct. Mater.*, 2019, **29**, 1902987.
2. Z. Chen, C. Hao, B. Yan, Q. Chen, H. Feng, X. Mao, J. Cen, Z. Q. Tian, P. Tsiakaras and P. K. Shen, *Adv. Energy Mater.*, 2022, **12**, 2201600.
3. Y. Liu, C. Zhan, J. Zhang, X. Huang and L. Bu, *J. Mater. Chem. A*, 2023, **11**, 1455-1460.
4. K. Wan, J. Wang, J. Zhang, B. Li, M. Chai, P. Ming and C. Zhang, *Chem. Eng. J.*, 2024, **482**, 149060.
5. W. Xu, Z. Zhu, Y. Wang, P. Cui, L. Tong, K. Zhao, J. Yuan, Z.-Y. Zhou, H.-W. Liang, N. Tian and S.-G. Sun, *J. Mater. Chem. A*, 2023, **11**, 4078-4087.
6. J. Chen, G. Qian, B. Chu, Z. Jiang, K. Tan, L. Luo, B. Li and S. Yin, *Small*, 2022, **18**, 2106773.
7. W. Liao, S. Zhou, Z. Wang, J. Long, M. Chen, Q. Zhou and Q. Wang, *J. Mater. Chem. A*, 2022, **10**, 21416-21421.
8. Y. Nie, J. Deng, W. Jin, W. Guo, G. Wu, M. Deng, J. Zhou, R. Yang, S. Zhang and Z. Wei, *J. Alloys Compd.*, 2021, **884**, 161063.
9. N. Zhou and Y. Li, *Int. J. Hydrogen Energy*, 2021, **46**, 37884-37894.
10. S. Zhu, Y. Liu, Y. Gong, Y. Sun, K. Chen, Y. Liu, W. Liu, T. Xia, Q. Zheng, H. Gao, H. Guo and R. Wang, *Small*, 2023, **20**, 2305062.